RESEARCH ARTICLE

Inhibition of BACE1, the β-secretase implicated in Alzheimer's disease, by a chondroitin sulfate extract from *Sardina pilchardus*

Courtney J. Mycroft-West[1], Anthony J. Devlin[1], Lynsay C. Cooper[1], Patricia Procter[1], Gavin J. Miller[2], David G. Fernig[3], Marco Guerrini[4], Scott E. Guimond[5, 1, 3], Marcelo A. Lima[1], Edwin A. Yates[3, 1], Mark Andrew Skidmore[1, 3, 5, *]

1 Molecular & Structural Biosciences, School of Life Sciences, Keele University, Huxley Building, Keele, Staffordshire, ST5 5BG, UK
2 Lennard-Jones Laboratory, School of Chemical and Physical Sciences, Keele University, Keele, Staffordshire, ST5 5BG, UK
3 Department of Biochemistry, Institute of Integrative Biology, University of Liverpool, Crown Street, Liverpool, L69 7ZB, UK
4 Istituto di Ricerche Chimiche e Biochimiche G. Ronzoni, Via G. Colombo 81, 20133 Milan, Italy
5 School of Medicine, Keele, Staffordshire, ST5 5BG, UK

Funding: *This study was financially supported by grants from the Engineering and Physical Sciences Research Council, UK, the Biotechnology and Biological Sciences Research Council, UK, the Medical Research Council, UK, Intellihep Ltd., UK, MI Engineering Ltd., UK and Financiadora de Estudos e Projetos.*

Abstract

The pharmaceutical and anticoagulant agent heparin, a member of the glycosaminoglycan family of carbohydrates, has previously been identified as a potent inhibitor of a key Alzheimer's disease drug target, the primary neuronal β-secretase, β-site amyloid precursor protein cleaving enzyme 1 (BACE1). The anticoagulant activity of heparin has, however, precluded the repurposing of this widely used pharmaceutical as an Alzheimer's disease therapeutic. Here, a glycosaminoglycan extract, composed predominantly of 4-sulfated chondroitin sulfate, has been isolated from *Sardina pilchardus*, which possess the ability to inhibit BACE1 (IC_{50} [half maximal inhibitory concentration] = 4.8 μg/mL), while displaying highly attenuated anticoagulant activities (activated partial thromboplastin time EC_{50} [median effective concentration] = 403.8 μg/mL, prothrombin time EC_{50} = 1.3 mg/mL). The marine-derived, chondroitin sulfate extract destabilizes BACE1, determined via differential scanning fluorimetry (ΔT_m –5°C), to a similar extent as heparin, suggesting that BACE1 inhibition by glycosaminoglycans may occur through a common mode of action, which may assist in the screening of glycan-based BACE1 inhibitors for Alzheimer's disease.

Key Words: *amyloid-β; aspartyl protease; carbohydrates; galactosaminoglycans; heparan sulfate; heparin; marine polysaccharide; pilchards; sardines; therapeutics*

Chinese Library Classification No. *R453; R364; R741*

***Correspondence to:**
Mark Andrew Skidmore, PhD,
m.a.skidmore@keele.ac.uk.

orcid:
0000-0002-0287-5594
(Mark Andrew Skidmore)

doi: *10.4103/1673-5374.274341*

Received: *August 9, 2019*
Peer review started: *August 23, 2019*
Accepted: *October 26, 2019*
Published online: *January 31, 2020*

Introduction

The largest cause of dementia worldwide, Alzheimer's disease (AD), results from the gradual cerebral atrophy of brain regions associated with learning and memory (Lane et al., 2017). Existing therapeutics licensed for treatment are palliative in nature, and do not target the underlying disease aetiology (Coimbra et al., 2018). It has therefore, become a focus to develop a therapeutic agent capable of targeting the underlying disease mechanisms of AD in order to preclude neurodegeneration before symptoms manifest.

In addition to the defining hallmarks of AD, amyloid-β (Aβ) plaques and intraneuronal neurofibrillary tangles (Querfurth and LaFerla, 2010), other pathophysiologies of AD include neurotransmitter depletion, apolipoprotein E polymorphism, oxidative stress, inflammation and mitochondrial dysfunction. A common linked factor is the accumulation of Aβ peptides, the principal component of Aβ plaques (Rashid et al., 2018). Consequently, limiting the overproduction of Aβ has become an attractive target for halting AD. Aβ results from amyloid precursor protein (APP) metabolism through the amyloidogenic pathway, which commences by the catalytic action of the β-site amyloid precursor protein-cleaving enzyme 1 (BACE1). Cleavage of the resulting C-terminal APP fragment, β-carboxyl terminal fragment, by γ-secretase releases Aβ peptides of variable lengths into the extracellular space, where oligomerization can occur (Querfurth and LaFerla, 2010). Cleavage of APP by BACE1 is therefore, the rate-limiting step of Aβ production, and as such has become a leading drug target for AD (Vassar, 2016; Coimbra et al., 2018).

Glycosaminoglycans (GAGs) are anionic, linear heteropolysaccharides, which differ by the constituent disaccharide repeat units of either an uronic acid (D-glucuronic acid, GlcA or L-iduronic acid, IdoA), or D-galactose (Gal), and an amino sugar (D-galactosamine [GalN] or D-glucosamine [GlcN]) (Gandhi and Mancera, 2008). Structural differences between disaccharide repeat regions give rise to four main GAG classes: chondroitin sulfate (CS)/dermatan sulfate (DS), heparin/heparan sulfate (HS), keratan sulfate, and hyaluronic acid (HA). Each monosaccharide within the disaccharide

unit may possess distinct degrees, and positions, of sulfation that dictate their biological activities (Powell et al., 2004), e.g., the potent anticoagulant activity of heparin, widely used as a clinical anticoagulant, is attributed principally to the pentasaccharide sequence [–4) α-D-GlcNS,6S (1–4) β-D-GlcA (1–4) α-D-GlcNS,3S,6S (1–4) α-L-IdoA2S (1–4) α-D-GlcNS,6S (1–] (Mulloy et al., 2016), although this example, does not typify the complexity of GAG structure-function relationships since several structures exhibit different levels of activity.

Previously, the GAGs HS and heparin have been identified as potent inhibitors of BACE1 (Scholefield et al., 2003; Patey et al., 2006, 2008; Schwörer et al., 2013; Zhang et al., 2016). Low molecular weight GAGs have also been shown to possess the ability to cross the blood-brain barrier while retaining the ability to inhibit BACE1 (Leveugle et al., 1998; Patey et al., 2006), which proves a challenge for many small molecule inhibitors (Vassar, 2016). Despite this, the repurposing of heparin and low molecular weight derivatives (low molecular weight heparins) as a treatment for AD is largely prohibited by the likely side effect of anticoagulation. It has been demonstrated that simple chemical modifications can ablate the anticoagulant activity of heparin, while retaining favorable bioactivities such as BACE1 inhibition (Patey et al., 2006, 2008). A number of polysaccharides have been isolated from marine species, which share the underlying disaccharide backbone of GAGs, however, display unique structural modifications compared to their mammalian counterparts. As an account of the structural diversity of marine GAGs, many have been observed to possess favorable bioactivities while exhibiting a diminished effect on anticoagulation compared to mammalian heparin (Valcarcel et al., 2017; Mycroft-West et al., 2018). Furthermore, the therapeutic exploitation of these marine-GAGs may be advantageous over their mammalian counterparts due to religious beliefs, are unlikely to be contaminated by mammalian pathogens (e.g., spongiform encephalopathies), and can be acquired from aquaculture waste, making their exploitation economically, environmentally and socially appealing. Previously, a heparin/HS-like GAG extracted from *Portunus pelagicus*, was demonstrated to inhibit BACE1 (Mycroft-West et al., 2019). Here, a further GAG extract, composed primarily 4-sulfated CS (CSA), isolated from *Sardina pilchardus* (*S. pilchardus*), was screened for the ability to inhibit BACE1.

Materials and Methods

Glycosaminoglycans extraction

The CSA containing, GAG extract from *S. pilchardus* was isolated essentially as described by Mycroft-West et al. (2019). Briefly 3.4 kg of *S. pilchardus* tissue (Oceana Group Company Lucky Star, Cape Town, South Africa) was delipidated by homogenisation in excess acetone (VWR, Lutterworth, UK). After 24 hours, excess acetone was removed via centrifugation and the recovered tissue dried prior to protease digestion (Alcalase®; Novozymes, Denmark) at 60°C for 24 hours. Glycosaminoglycan capture was facilitated using Amberlite ion exchange resin (IRA-900; Sigma-Aldrich, Dorset, UK; OH^- form), which underwent extensive washes (1 M NaCl) prior to elution (3 M NaCl). Glycosaminoglycans were subsequently precipitated (4°C for 48 hours) by the addition of methanol (1:1 v/v, 4°C; VWR, Lutterworth, UK) and desalted by dialysis utilizing a 3.5 kDa MWCO membrane (48 hours; Biodesign, Carmel, NY, USA) against distilled H_2O. The crude GAG extract was fractionated by DEAE-Sephacel (GE Healthcare, Buckinghamshire, UK) high-pressure, ion exchange liquid chromatograph (HPELC; Cecil Instruments, Cambridge, UK) post-filtration (0.2 μm, nylon syringe filter, Fisher Scientific, Loughborough, UK). Elution was performed with a stepwise high pressure liquid chromatography (HPLC) grade sodium chloride gradient 0, 0.25, 0.5, 0.8, 1 and 2 M NaCl (fractions F1–F6, respectively; Fisher Scientific) at a flow rate of 2 mL/min with inline UV-detection (λ_{abs} = 232 nm). Eluted fractions were extensively dialyzed against distilled H_2O, utilizing a 3.5 kDa MWCO membrane (Biodesign) and subsequently lyophilized. Samples were stored at 4°C until required.

Agarose gel electrophoresis

S. pilchardus extract (2–10 μg) alongside *bona fide* GAG standards (CSA, CSC, DS, heparin and HS) were subjected to electrophoretic separation using a 0.55% (w/v) agarose gel-based medium (80 × 80 × 1.5 mm) prepared in 50 mM 1,3-diaminopropane-acetate (PDA) buffer, pH 9.0 (VWR), using a X-Cell SureLock™ Mini-Cell Electrophoresis System (ThermoFisher, Loughborough, UK). Electrophoresis was carried out for 30 minutes at 150 V, in PDA buffer, pH 9.0. Fixation was performed using 0.1% (w/v, aqueous) cetyltrimethylammonium bromide (VWR) for 60 minutes prior to staining with 0.1% (w/v) toluidine blue (Fisher Scientific) in acetic acid:ethanol: H_2O (0.1:5:5, v/v). Gels were destained in the same solution, with the omission of toluidine blue (Fisher Scientific) prior to processing using GIMP (v2.8, Berkeley, CA, USA) and ImageJ software (v1.51 (100), National Institutes of Health, Bethesda, MD, USA), as previously reported (Mycroft-West et al., 2019).

Attenuated total reflectance fourier transform infrared spectroscopy

The attenuated total reflectance fourier transform infrared (ATR-FTIR) spectra of lyophilized carbohydrate samples (5 mg) were recorded as reported in Devlin et al. (2019) using a Bruker Alpha I spectrometer (between 400 to 4000 cm^{-1}; 2/cm resolution) and have been presented as an average of 5 replicates (32 scans each). Background spectra were acquired prior to each sample and subtracted from the sample spectra in order to correct for features derived from the sampling environment. All ATR-FTIR spectra were processed using a Savitzky-Golay smoothing algorithm (R studio v1.1.463; signal package, sgolayfilter),

to a 2nd degree polynomial with 21 neighbours. Following smoothing baseline correction employing a 7th-order polynomial was performed to negate any additional fluctuations in atmospheric conditions during sample spectra acquisition. Spectra were subsequently normalized between 0 and 1 to account for any variation in sample quantity in contact with the ATR crystal. Spectral processing was conducted on an Asus Vivobook Pro fitted with an i7-7700HQ processor (M580VD-EB76, Taipet, Taiwan, China). The CO_2 and H_2O regions were omitted in order to negate environmental variability (2000–2500 cm^{-1}, > 3600 cm^{-1} and < 700 cm^{-1}), as described previously (Devlin et al., 2019; Mycroft-West et al., 2019). Spectra were subsequently analyzed using principal component analysis.

Circular dichroism

The circular dichroism spectra of *S. pilchardus* extract and *bona fide* GAG standards in HPLC grade H_2O (10 mg/mL), were recorded (1 nm resolution, λ = 250 to 190 nm, 3 accumulations) using a Jasco J-1100 spectrometer (JASCO, Inc., Oklahoma City, Oklahoma, USA) equipped with a quartz based sample-cell (0.2 mm path length; Hellma, Plainview, NY, USA) calibrated with (+)-10-camphorsulfonic acid (1 mg/mL). A baseline of HPLC grade H_2O was recorded prior to sample acquisition, utilizing identical settings, and subtracted from sample spectra. Prior to statistical analysis using principal component, analysis spectra were normalized to 250 nm.

Nuclear magnetic resonance

Nuclear magnetic resonance (NMR) experiments were carried out on the *S. pilchardus* CSA extract (5 mg in D_2O; Alfa Aesar) at 298 K utilizing a Neo spectrometer (800-MHz; TCI cryoprobe; Bruker, Coventry, UK). Two-dimensional heteronuclear single-quantum coherence (^1H–^{13}C) spectra were recorded with standard gradient pulse sequences employing non-uniform sampling. Spectral processing was performed using TopSpin (Bruker).

Förster resonance energy transfer

The *S. pilchardus* extract and porcine mucosal heparin (PMH) were screened for inhibitory against human β-secretase (tag-free BACE1; ACRO Biosystems, Cambridge, MA, USA) utilizing a method modified from that of Patey et al. (2006) employing the principle of Förster resonance energy transfer (FRET). Human BACE1 (312.5 ng) was pre-incubated with *S. pilchardus* CSA, PMH in sodium acetate buffer (50 mM, pH 4.0) at 37°C for 10 minutes, prior to addition of a quenched fluorogenic, peptide substrate, pre-incubated at 37°C (MCA-SEVNLDAEFRK[DNP]RR-NH2; 6.25 μM; Biomatik, Cambridge, Canada), to a final well volume of 100 μL. Substrate only (containing no BACE1) and H_2O controls were employed in order to define 100% and 0% inhibition, respectively. Fluorescent emission was monitored for 90 minutes at $\lambda_{exc/emm}$ = 320:405 nm on a Tecan Infinite® M200-Pro plate reader (Tecan Group Ltd., Männedorf, Switzerland) equipped with i-control™.

Differential scanning fluorimetry

Differential scanning fluorimetry (DSF) was performed using the method of Uniewicz et al. (2010), post adaption from Niesen et al. (2007). *S. pilchardus* CSA, heparin (Celsus, Cincinnati, OH, USA; maximum concentration of 200 μg/mL) or H_2O were incubated with human BACE1 (1 μg) with 20 × Sypro Orange (Invitrogen), in 50 mM sodium acetate, pH 4.0 to make a final volume of 40 μL in 96-well qPCR plates (AB Biosystems, Warrington, UK). ΔRFu was monitored on a StepOne plus qPCR machine (AB Biosystems) using the TAMRA filter, thermal melt curves were recorded between 20–90°C with an initial incubation phase of 2 minutes at 20°C, before increasing + 0.5°C increments every 30 seconds.

Activated partial thromboplastin time

S. pilchardus extract, PMH samples (25 μL) or control (H_2O, HPLC grade) were mixed prior to incubation with normal human plasma (50 μL, pooled & citrated; Technoclone, Surrey, UK) and Pathromtin SL (50 μL; Siemens, Erlangen, Germany) at 37°C for 120 seconds in advance of the addition of $CaCl_2$ (50 mM; 25 μL, Alfa Aesar, Heysham, UK). The time taken for clot formation was noted using a coagulometer (Thrombotrak Solo; 120 second upper maximum for 100% clotting; Axis-Shield) as described by Mycroft-West et al. (2019). Mucosal heparin (porcine, 193 IU/mg; Celsus) and HPLC-grade H_2O (clotting time of 37–40 seconds, representing 0% inhibition) were used as controls.

Prothrombin time

S. pilchardus extract, PMH (50 μL) or H_2O control (HPLC grade were mixed prior to incubation with normal human plasma (50 μL, pooled & citrated; Technoclone) at 37°C for 60 seconds in advance of the insertion of Thromborel S (50 μL; Siemens). The time taken for clot formation was noted using a coagulometer (Thrombotrak Solo, Axis-Shield, Dundee, UK; 120-second upper maximum for 100% clotting;) as described by Mycroft-West et al. (2019). Mucosal heparin (porcine, 193 IU/mg; Celsus) and HPLC-grade H_2O (clotting time of 13–14 seconds, representing 0% inhibition) were used as controls.

Statistical analysis

Principal component analysis was applied to normalized FTIR and circular dichroism spectra, using the singular value decomposition (SVN), *base prcomp* function in R (v1.1.463, R studio Inc. Boston, MA, USA; installed upon an Asus Vivobook Pro fitted with an i7-7700HQ processor M580VD-EB76) as described previously (Devlin et al 2019; Mycroft-West et al., 2019). The matrices of intensities were mean-centred, with no additional scaling. Scree plots indicated the principal components displaying the greatest variance.

Percentage BACE1 inhibition for FRET assays were cal-

culated by determining fluorescence change (ΔRFu/min) for all samples within the linear-range of the 0% inhibition control. Percentage inhibition was subsequently calculated relative to ΔRFu/min of 0 and 100% inhibition controls (n = 3; ± SD). Data has been fitted using non-linear regression (four-parameter logistics model) to determine IC_{50} values, using GraphPad Prism 7 (GraphPad Software, San Diego, CA, USA).

Melting temperatures (T_m) of BACE1 were determined by smoothing melt curves (19 neighbours, Savitzky-Golay 2nd order polynomial) obtained from DSF experiments and plotting the first derivative (GraphPad Prism 7). The peak maxima of the first-derivative plots (T_m; n = 3; ± SD) were determined using MatLab (R20018a; MathWorks, Cambridge, UK).

EC_{50}s for activated partial thromboplastin time (aPTT) and prothrombin time (PT) assays (n = 3; ± SD) were obtained using Prism 7 (sigmoidal, dose response; GraphPad Software).

Results

Isolation and characterization of a chondroitin sulfate A extract from *S. pilchardus*

A crude GAG extract was obtained from *S. pilchardus* by proteolytic digestion, as previously described (Mycroft-West et al., 2019), and subsequently isolated with anion-exchange chromatography (Sephacel DEAE) employing a NaCl, stepwise gradient. The eluate obtained in the 800 mM NaCl fraction (F4), was analyzed by agarose-based, electrophoresis using a PDA buffer system. Fraction 4 (F4) of the *S. pilchardus* GAG extract possessed comparable electrophoretic migration to that of chondroitin and/or dermatan sulfate (DS). The bands observed did not correspond with the migration of mammalian heparin or HS (**Figure 1**).

The ATR-FTIR spectrum of *S. pilchardus* F4 was compared with that of a library of bone fide GAGs using principal component analysis (**Figure 2**). PC1 and PC2 were compared (comprising 72% of the variance), separating *S. pilchardus* F4 into the CSA containing region, which is distinct from other GAGs (**Figure 2B**).

Principal component analysis was further employed to compare the circular dichroism spectra of *S. pilchardus* F4 with that of known GAGs (**Figure 3**). Glycosaminoglycan circular dichroism spectra are particularly sensitive to uronic acid conformation (Rudd et al., 2009), while CS and DS differ in their composition incorporating either GlcA or IdoA, respectively. Heparin also contains higher levels of IdoA relative to HS (Meneghetti et al., 2015). Comparison of PC1 (covering 87.6% of the total variance) separated *S. pilchardus* F4 away from heparin/HS samples and into a region alongside CS/DS. While comparison of PC1 versus PC2 (covering 97.4% of the total variance) further separates CS from DS samples, with *S. pilchardus* F4 aligning within the CS cluster.

S. pilchardus F4 was confirmed to be predominantly CSA by two-dimensional heteronuclear single quantum coherence NMR. Spectra revealed the principal N-acetyl region (^{1}H) at 2.02 ppm, corresponding to that of CS (Gardini et al., 2017) with a minor peak at 2.08 ppm (^{1}H) also observed, characteristic of DS (Gardini et al., 2017) (**Figure 4**). Integration of the N-acetyl stretches corresponding to CS and DS indicated that the GAG component of *S. pilchardus* F4 is composed of > 95% CS. Furthermore, integration of the regions corresponding to A2 and A6 indicated that the *S. pilchardus* F4 sample contained sulfation at predominantly the C4 position of the N-acetyl galactosamine residue. Minor peaks that could be associated to other GAGs and/or different CS substitution pattern are also observed but these are of very low intensity. Together, the data suggest that *S. pilchardus* F4 is CSA-like in nature and from herein, will be referred to as a *S. pilchardus* CSA extract.

A CSA extract from *S. pilchardus* inhibits the human β-secretase, BACE1

The BACE1 inhibitory potential of both the *S. pilchardus* CSA extract and PMH (with known inhibitory activity) was assayed using FRET (Scholefield et al., 2003; Patey et al., 2006; Mycroft-West et al., 2019). The *S. pilchardus* CSA extract exhibited maximal inhibition at concentrations greater than 10 μg/mL; IC_{50} = 4.8 μg/mL with an R^2 of 0.93, approximately 2-fold lower than that of PMH (IC_{50} = 2.6 μg/mL; R^2 = 0.97, **Figure 5**). Chondroitin sulfate has previously been reported to possess only weak BACE1 inhibitory activity by Scholefield et al. (2003), however, the specific structural composition, in regards of the total sulfation level or pattern, has not been reported.

Human β-secretase (BACE1) is destabilized by the presence of the *S. pilchardus* CSA extract

DSF was utilized to determine whether the extract form *S. pilchardus* CSA altered the thermal stability of BACE1 in a similar fashion to PMH (Mycroft-West et al., 2019). A 1:4 ratio (w/w) of BACE1:PMH the thermal stability of BACE1 decreased by ΔT_m = –10.5°C (± 0.5 SD, n = 3), in line with previous reports (**Figure 6A**) (Mycroft-West et al., 2019). In contrast, in the presence of the *S. pilchardus* CSA extract at the same w/w ratio (1:4, BACE1:*S. pilchardus* CSA) the ΔT_m of BACE1 = –5°C (± 1.3 SD, n = 3), an approximately 2-fold reduction in the level of thermal destabilization compared to that of PMH. The destabilization of BACE1 by both PMH and the *S. pilchardus* CSA extract demonstrated concentration dependence (**Figure 6B**).

The *S. pilchardus* CSA extract exhibits negligible aPTT and PT anticoagulation activities

The anticoagulant activity of heparin would appear to preclude its use as a pharmaceutical against alternative disease states such as AD. With the exception of chemically over-sulfated chondroitin sulfate, native CS possesses negligible anticoagulant activity compared to that of mammalian heparin (Hogwood et al., 2018). To verify this, the activities

of *S. pilchardus* CSA in the aPTT (intrinsic pathway) and PT (extrinsic pathway) assays were examined against the known clinical anticoagulant, PMH (193 IU/mg). *S. pilchardus* CSA displayed a > 200 fold reduction in the aPTT (**Figure 7A**) with an EC_{50} of 403.8 μg/mL compared to PMH (EC_{50} = 1.6 μg/mL) and greater than an 80 fold reduction in the PT (**Figure 7B**) with an EC_{50} of 1.3 mg/mL when compared to PMH (EC_{50} = 14.8 μg/mL). Both coagulation assays indicate that the *S. pilchardus* CSA possesses negligible anticoagulant activity.

Discussion

The GAG extract obtained from *S. pilchardus* was identified to have comparable electrophoretic migration to that of CS/DS when subject to agarose-based, PDA buffered, gel electrophoresis. Further spectroscopic analysis of the *S. pilchardus* extract suggested that the major GAG composition falls within that of CS, with the FTIR further aligning towards CS sulfated predominantly at the C4 position (CSA). Two-dimensional heteronuclear single quantum coherence NMR, revealed that the principal N-acetyl signal corresponded to that of CS, with the majority of the CS component containing 4-O-sulfated GalNAc residues. Minor spectral features were also observed but, with very low intensity, suggesting they account for < 5% of the extract.

The *S. pilchardus* CSA extract exhibited inhibitory potential against BACE1 in a manner similar to PMH albeit at a slightly diminished level, as demonstrated by the IC_{50} (determined via dose-response FRET assays). This is in contrast to previous observations that CS does not exhibit BACE1 inhibitory activity above ~20%, however, the fine structure of the CS was not reported in this study (Scholefield et al., 2003). This indicates that BACE1 inhibitory activity of CS may require sulfation at defined positions rather than as a result of total anionic charge, as previously identified for HS/heparin (Patey et al., 2006). A decrease in the thermal stability of BACE1, was also observed by DSF (T_m values) in the presence of PMH or the *S. pilchardus* CSA extract, as previously reported for the glucosaminoglycans (Mycroft-West et al., 2019). The ability of heparin and the *S. pilchardus* CSA extract to promote thermal destabilization of BACE1 occurred with a concentration-dependent response similar to that of the inhibitory potential in FRET-based assays. A comparable two-fold decrease in the IC_{50} required for BACE1 inhibition (FRET) and in ΔT_m (DSF) was observed in the presence of *S. pilchardus* CSA extract compared to PMH. This suggests that the mode of BACE1 inhibition by the GAG category of carbohydrates may involve structural destabilization, in contrast to other known BACE1 inhibitors, for which stabilization has been reported using the same technique (Lo et al., 2004). Destabilization of BACE1 by GAGs would appear to be linked directly to BACE1 inhibitory potential, for this class of molecules.

The repurposing of heparin-derived pharmaceuticals as potential BACE1 inhibitors, or for other alternative therapeutics is largely precluded by significant anticoagulant potential owing to its inhibition of the human coagulation cascade, primarily through antithrombin III. With the notable exception of over-sulfated chondroitin sulfate, which is not naturally occurring, CS exhibits negligible anticoagulant activity in comparison to mammalian heparin (Hogwood et al., 2018). The anticoagulant potential of the *S. pilchardus* CSA extract was, therefore, examined using the aPTT and PT coagulation assays, which are widely used to examine the intrinsic or extrinsic pathways, respectively. It should be noted that both assays incorporate the common pathway. The *S. pilchardus* CSA extract displayed highly attenuated activity compared to PMH in both the aPTT and PT assays. Despite the slightly diminished BACE1 inhibitory activity of the *S. pilchardus* CSA extract in comparison to unmodified PMH, the therapeutic value is greater when anticoagulation activity is taken into account. In addition to heparin, CS is also available as either an over the counter neutraceutical (USA) or, as a prescribed drug under the European Medical Agency for the treatment of osteoarthritis (Herotin et al., 2010). Current CS drugs are considered to show no significant side effects (Herotin et al., 2010), in contrast to heparin pharmaceuticals, whose well-known side effect is heparin-induced thrombocytopenia. In addition, CS has been reported to be bioavailable through oral and subcutaneous routes (for review of the pharmacokinetic properties of CS see Heroti et al., 2010), whereas heparin is not absorbed after oral administration without the requirement of additional formulations (Mousa et al., 2014). The development of a CS based therapeutic for AD may therefore offer additional advantages over other GAGs, and small peptide inhibitors, which have unfavorable pharmacokinetic properties (Vassar, 2016).

The utilization of marine derived GAGs for the discovery of novel bioactive compounds is advantageous over other mammalian sources currently being explored (for both heparin and CS therapeutics), as many marine species such as, *S. pilchardus* overcome religious mores and are free from mammalian pathogens (e.g., spongiform encephalopathies, swine viruses). Glycosaminoglycans can also be obtained readily from marine aquaculture waste material and in some cases can be farmed in a controlled aquaculture environment, making their exploitation economically and environmentally favorable, whilst constituting a sustainable source of biologically active glycans. The exploitation of marine species as a novel source of bioactive GAGs is therefore an attractive alternative to the mammalian sources that are currently utilized to obtain GAGs for therapeutic use.

Author contributions: *Study concept: CJM, LCC, DGF, SEG, EAY, MAS; study design: CJM, LCC, DGF, SEG, MAL, EAY, MAS; critical revision of the manuscript for important intellectual content: CJM, MAS; literature search: CJM, EAY, MAS; experiment implementation: CJM, AJD, LCC, PP, MAL, MAS; statistical analysis: CJM, AJD; manuscript editing: CJM, AJD, LCC, SEG, MAL, EAY, MAS; manuscript review: PP, GJM, DGF, MG, SEG, MAL, EAY, MAS; data acquisition: CJM, AJD, LCC, PP, MG, MAL, MAS; data analysis: CJM, AJD, LCC, PP, GJM, MG, SEG, MAL,*

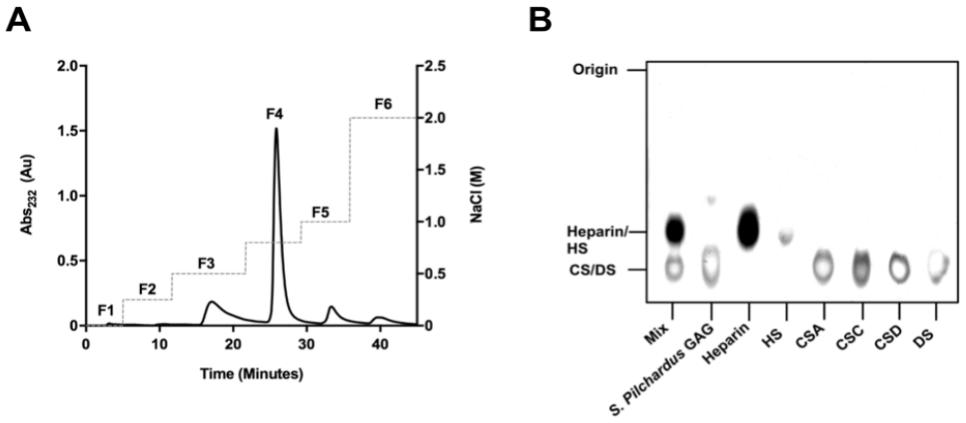

Figure 1 Separation of the crude *S. pilchardus* glycosaminoglycan extract by anion-exchange chromatography and agarose-based gel electrophoresis.
(A) Anion exchange chromatogram of crude *S. pilchardus* glycosaminoglycan extract. Fractions 1–6 (denoted F1–6) were eluted with a NaCl gradient (dashed line) with elution monitored at λ_{Abs} of 232 nm (solid line). (B) Electrophoretic mobility of the glycosaminoglycan (GAG) extract from *S. pilchardus* (F4; 800 mM) compared against *bona fide* glycosaminoglycans of heparin, heparan sulfate (HS), chondroitin sulfate A (CSA), C (CSC) and D (CSD), and dermatan sulfate (DS). Mix = chondroitin sulfate A, heparin and heparan sulfate mixture.

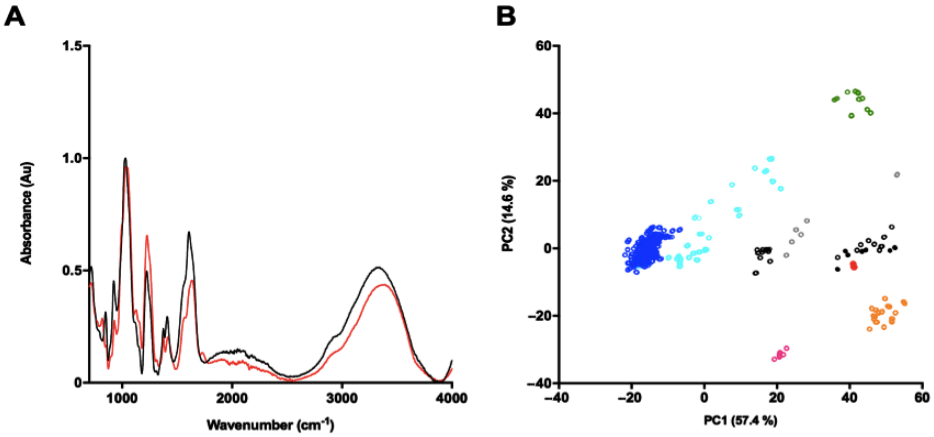

Figure 2 Attenuated total reflection Fourier-transform infrared spectrum of the crude *S. pilchardus* glycosaminoglycan extract.
(A) Chondroitin sulfate A (black) and *S. pilchardus* (red) attenuated total reflection Fourier-transform infrared spectra, $n = 5$. (B) Principal component analysis Score Plot (PC1 *vs.* PC2) of *S. pilchardus* compared against a *bone fide* glycosaminoglycan library. Heparan sulfate (cyan), heparin (blue), chondroitin sulfate with composition not stated (black, open circles), chondroitin sulfate A (black filled circles), chondroitin sulfate C (grey), dermatan sulfate (orange), over-sulfated chondroitin sulfate (magenta), hyaluronic acid (green), *S. pilchardus* glycosaminoglycans (red filled circles).

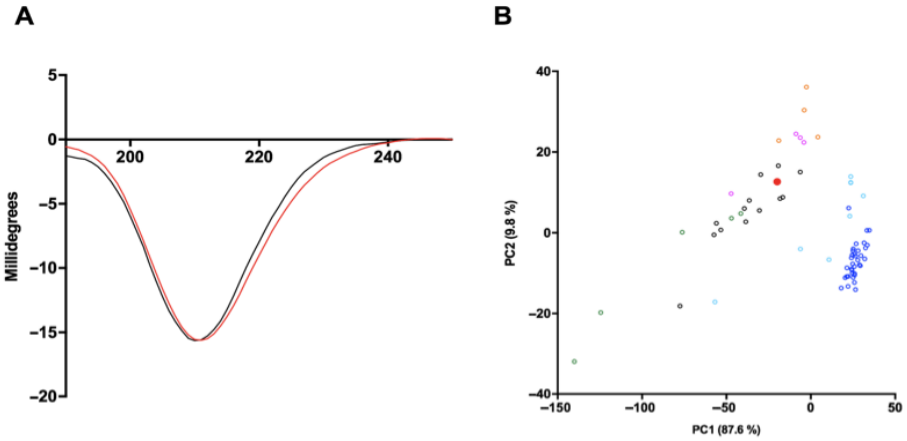

Figure 3 Circular dichroism spectrum of the crude *S. pilchardus* glycosaminoglycan extract.
(A) Circular dichroism spectra of chondroitin sulfate A (black) and *S. pilchardus* (red). (B) Principal component analysis Score Plot (PC1 v. PC2) of *S. pilchardus* compared against a bone fide glycosaminoglycan library. Heparan sulfate (cyan), chondroitin sulfate (black), chondroitin sulfate A (black filled circles), heparin (blue), dermatan sulfate (orange), over sulfated chondroitin sulfate (magenta), hyaluronic acid (green), *S. pilchardus* glycosaminoglycan (red filled circle).

EAY, MAS; statistical analysis: CJM, AJD, EAY; manuscript preparation: CJM, AJD, EAY, MAS; study supervision: MAS. All authors approved the final manuscript.

Conflicts of interest: *None declared.*

Financial support: *This study was financially supported by grants from the Engineering and Physical Sciences Research Council, UK, the Biotechnology and Biological Sciences Research Council, UK, the Medical Research Council, UK, Intellihep Ltd., UK, MI Engineering Ltd., UK (and Financiadora de Estudos e Projetos. The funders did not have any role in the study design, data collection and interpretation, or the decision to submit this work for publication.*

Data sharing statement: *Datasets analyzed during the current study are available from the corresponding author on reasonable request.*

Plagiarism check: *Checked twice by iThenticate.*

Peer review: *Externally peer reviewed.*

Open peer reviewers: *Isaac G. Onyango, Gencia Biotechnology, USA; Hailong Song, University of Pennsylvania, USA.*

References

Coimbra JRM, Marques DFF, Baptista SJ, Pereira CMF, Moreira PI, Dinis TCP, Santos AE, Salvador JAR (2018) Highlights in BACE1 inhibitors for Alzheimer's disease treatment. Front Chem 6:178.

Devlin A, Mycroft-West C, Guerrini M, Yates E, Skidmore M (2019) Analysis of solid-state heparin samples by ATR-FTIR spectroscopy. bioRxiv:538074.

Gandhi NS, Mancera RL (2008) The structure of glycosaminoglycans and their interactions with proteins. Chem Biol Drug Des 72:455-482.

Gardini C, Urso E, Guerrini M, van Herpen R, de Wit P, Naggi A (2017) Characterization of danaparoid complex extractive drug by an orthogonal analytical approach. Molecules 22:1116.

Henrotin Y, Mathy M, Sanchez C, Lambert C (2010) Chondroitin sulfate in the treatment of osteoarthritis: from in vitro studies to clinical recommendations. Ther Adv Musculoskelet Dis 2:335-348.

Hogwood J, Naggi A, Torri G, Page C, Rigsby P, Mulloy B, Gray E (2018) The effect of increasing the sulfation level of chondroitin sulfate on anticoagulant specific activity and activation of the kinin system. PLoS One 13:e0193482.

Lane C, Hardy J, Schott JM (2017) Alzheimer's disease. Eur J Neurol 25:59-70.

Leveugle B, Ding W, Laurence F, Dehouck M P, Scanameo A, Cecchelli R, Fillit H (1998) Heparin oligosaccharides that pass the blood-brain barrier inhibit beta-amyloid precursor protein secretion and heparin binding to beta-amyloid peptide. J Neurochem 70:736-744.

Lo MC, Aulabaugh A, Jin G, Cowling R, Bard J, Malamas M, Ellestad G (2004) Evaluation of fluorescence-based thermal shift assays for hit identification in drug discovery. Anal Biochem 332:153-159.

Meneghetti MCZ, Hughes AJ, Rudd TR, Nader HB, Powell AK, Yates EA, Lima MA (2015) Heparan sulfate and heparin interactions with proteins. J R Soc Interface 12:20150589.

Mousa SA, Zhang F, Aljada A, Chaturvedi S, Takieddin M, Zhang H, Chi L, Castelli MC, Friedman K, Goldberg MM, Linhardt RJ (2007) Pharmacokinetics and pharmacodynamics of oral heparin solid dosage form in healthy human subjects. J Clin Pharmacol 47:1508-1520.

Mulloy B, Hogwood J, Gray E, Lever R, Page CP (2016) Pharmacology of heparin and related drugs. Pharmacol Rev 68:76-141.

Mycroft-West CJ, Cooper LC, Devlin AJ, Procter P, Guimond SE, Guerrini M, Fernig DG, Lima MA, Yates EA, Skidmore MA (2019) A glycosaminoglycan extract from portunus pelagicus inhibits BACE1, the β secretase implicated in Alzheimer's disease. Mar Drugs 17:293.

Mycroft-West CJ, Yates EA, Skidmore MA (2018) Marine glycosaminoglycan-like carbohydrates as potential drug candidates for infectious disease. Biochem Soc Trans 46:919-929.

Niesen FH, Berglund H, Vedadi M (2007) The use of differential scanning fluorimetry to detect ligand interactions that promote protein stability. Nat Protoc 2:2212-2221.

Patey SJ, Edwards EA, Yates EA, Turnbull JE (2006) Heparin derivatives as inhibitors of BACE-1, the Alzheimer's β-secretase, with reduced activity against factor Xa and other proteases. J Med Chem 49:6129-6132.

Patey SJ, Edwards EA, Yates EA, Turnbull JE (2008) Engineered heparins: novel beta-secretase inhibitors as potential Alzheimer's disease therapeutics. Neurodegener Dis 5:197-199.

Powell AK, Yates EA, Fernig DG, Turnbull JE (2004) Interactions of heparin/heparan sulfate with proteins: Appraisal of structural factors and experimental approaches. Glycobiology 14:17R-30R.

Querfurth HW, LaFerla FM (2010) Alzheimer's disease. N Engl J Med 362:329-344.

Rashid MMO, Paul SC, Halim MA, Aka TD (2018) A review on molecular neuropathology of Alzheimer s disease in association with aging. J Res Pharm 23:1-15.

Rudd T, Skidmore M, Guimond S, Holman J, Turnbull J, Lauder RM, Fernig DG, Yates EA (2009) The potential for circular dichroism as an additional facile and sensitive method of monitoring low-molecular-weight heparins and heparinoids. Thromb Haemost 102:874-878.

Scholefield Z, Yates EA, Wayne G, Amour A, McDowell W, Turnbull JE (2003) Heparan sulfate regulates amyloid precursor protein processing by BACE1, the Alzheimer's beta-secretase. J Cell Biol 163:97-107.

Schwörer R, Zubkova OV, Turnbull JE, Tyler PC (2013) Synthesis of a targeted library of heparan sulfate hexa- to dodecasaccharides as inhibitors of β-secretase: Potential therapeutics for Alzheimer's disease. Chemistry 19:6817-6823.

Uniewicz KA, Ori A, Xu R, Ahmed Y, Fernig DG, Yates E (2010) Differential Scanning Fluorimetry measurement of protein stability changes upon binding to glycosaminoglycans: a rapid screening test for binding specificity. Anal Chem 82:1-3.

Valcarcel J, Nova-Carballal R, Perez-Martin IR, Reis LR, Vazeuez AJ (2017) Glycosaminoglycans from marine sources as therapeutic agents. Biotechnol Adv 1:711-725.

Vassar R (2016) BACE1 inhibition as a therapeutic strategy for Alzheimer's disease. J Sport Heal Sci 5:388-390.

Zhang X, Zhao X, Lang Y, Li Q, Liu X, Cai C, Hao J, Li G, Yu G (2016) Low anticoagulant heparin oligosaccharides as inhibitors of BACE-1, the Alzheimer's β-secretase. Carbohydr Polym 151:51-59.

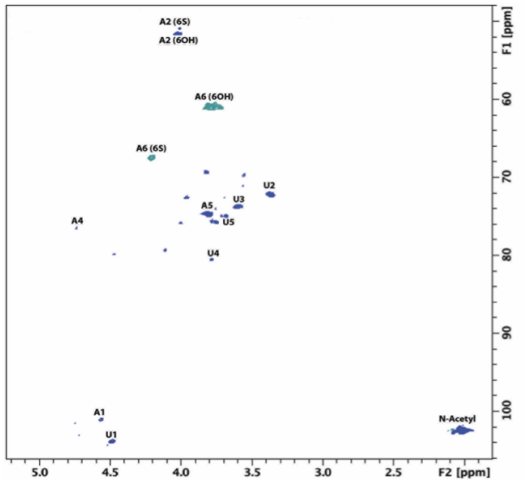

Figure 4 Nuclear magnetic resonance spectra (heteronuclear single quantum coherence) for *S. pilchardus* F4.
Chondroitin sulfate-associated major signals are indicated. Spectral integration was carried out using labelled signals. A: Galactosamine; U: uronic acid. Minor peaks are observed but with low intensity meaning that their abundance is lower than 5%. F1 and F2 are the indirect and direct dimensions, respectively.

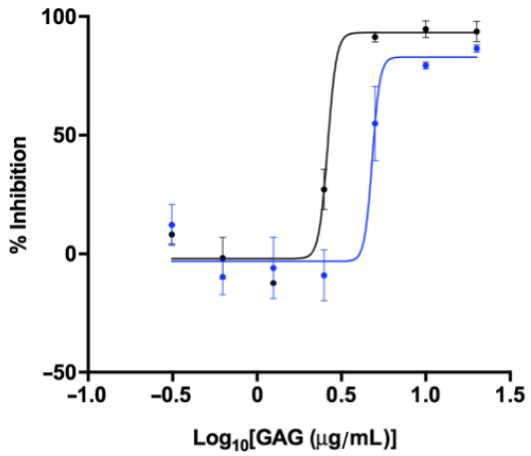

Figure 5 Inhibition of human beta-site amyloid precursor protein cleaving enzyme 1, by *S. pilchardus* chondroitin sulfate A (blue) or porcine mucosal heparin (black) as determined by Förster resonance energy transfer.
Porcine mucosal heparin IC_{50} = 2.6 µg/mL with an R^2 of 0.97; *S. pilchardus* chondroitin sulfate A extract IC_{50} = 4.8 µg/mL with an R^2 of 0.93. GAG: Glycosaminoglycan; IC_{50}: half maximal inhibitory concentration.

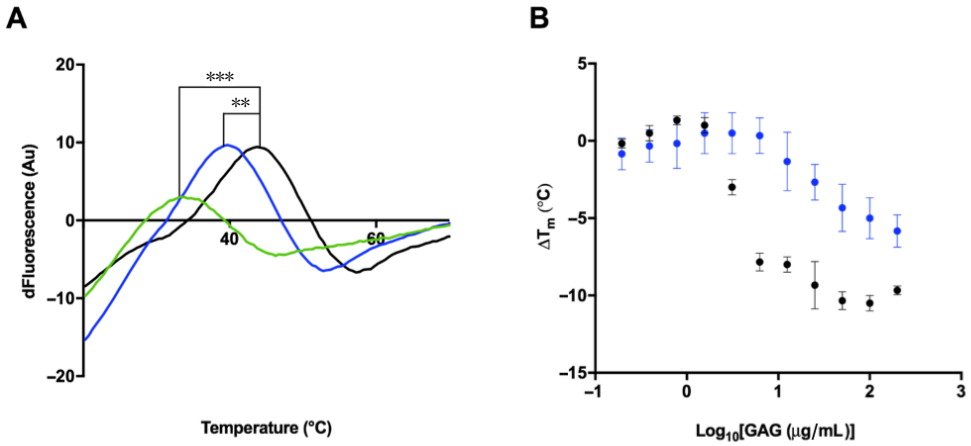

Figure 6 Differential scanning fluorimetry profile for the *S. pilchardus* chondroitin sulfate A extract.
(A) Thermal stability (first differential) profile of β-site amyloid precursor protein cleaving enzyme 1 (1 µg; black) and with 4 µg porcine mucosal heparin (green) or 4 µg *S. pilchardus* chondroitin sulfate A extract (blue), measured by differential scanning fluorimetry in 50 mM, pH 4.0, NaOAc buffer. ΔT_m of β-site amyloid precursor protein cleaving enzyme 1 with 4 µg of porcine mucosal heparin (*** –10.5°C ± 0.5 SD, *n* = 3) or 4 µg *S. pilchardus* chondroitin sulfate A extract (** –5°C ± 1.3 SD, *n* = 3). (B) ΔT_m of beta-site amyloid precursor protein cleaving enzyme 1 alone (black) or in the presence of increasing concentrations of porcine mucosal heparin or *S. pilchardus* chondroitin sulfate A extract.

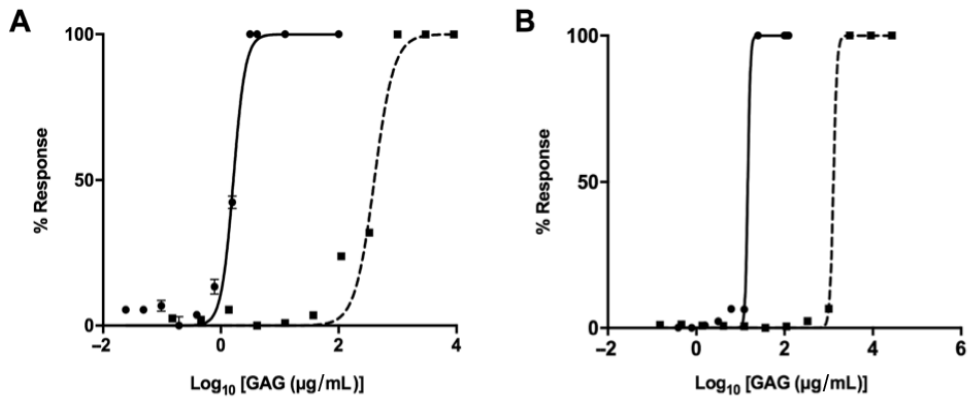

Figure 7 Anticoagulation profiles for the *S. pilchardus* chondroitin sulfate A extract.
Inhibitory response of heparin (circle, solid line) or *S. pilchardus* chondroitin sulfate A (square, dashed line) (mean % response, *n* = 3; ± SD) of (A) activated partial thromboplastin time (porcine mucosal heparin EC_{50} = 1.6 µg/mL, *S. pilchardus* chondroitin sulfate A EC_{50} = 403.8 µg/mL) and (B) Prothrombin time (porcine mucosal heparin EC_{50}= 14.8 µg/mL, *S. pilchardus* chondroitin sulfate A EC_{50} = 1.3 mg/mL).

P-Reviewers: Onyango IG, Song H; C-Editors: Zhao M, Li CH; T-Editor: Jia Y